

## Fast and slow domino regimes in transient network dynamics

Peter Ashwin,<sup>1,2</sup> Jennifer Creaser,<sup>1,2</sup> and Krasimira Tsaneva-Atanasova<sup>1,2,3</sup>

<sup>1</sup>*Department of Mathematics, University of Exeter, Exeter EX4 4QF, United Kingdom*

<sup>2</sup>*EPSRC Centre for Predictive Modelling in Healthcare, University of Exeter, Exeter EX4 4QJ, United Kingdom*

<sup>3</sup>*Living Systems Institute, University of Exeter, Exeter EX4 4QD, United Kingdom*

(Received 24 January 2017; published xxxxxx)

It is well known that the addition of noise to a multistable dynamical system can induce random transitions from one stable state to another. For low noise, the times between transitions have an exponential tail and Kramers' formula gives an expression for the mean escape time in the asymptotic limit. If a number of multistable systems are coupled into a network structure, a transition at one site may change the transition properties at other sites. We study the case of escape from a “quiescent” attractor to an “active” attractor in which transitions back can be ignored. There are qualitatively different regimes of transition, depending on coupling strength. For small coupling strengths, the transition rates are simply modified but the transitions remain stochastic. For large coupling strengths, transitions happen approximately in synchrony—we call this a “fast domino” regime. There is also an intermediate coupling regime where some transitions happen inexorably but with a delay that may be arbitrarily long—we call this a “slow domino” regime. We characterize these regimes in the low noise limit in terms of bifurcations of the potential landscape of a coupled system. We demonstrate the effect of the coupling on the distribution of timings and (in general) the sequences of escapes of the system.

DOI: [10.1103/PhysRevE.00.002300](https://doi.org/10.1103/PhysRevE.00.002300)

### I. INTRODUCTION

A number of important physical, biological, and socioeconomic questions involve understanding how a dynamical change of one subsystem within a network affects other subsystems that are coupled to it. Indeed, there is extensive work on noisy coupled bistable units, motivated by trying to understand the collective response and phase transitions. This includes work on stochastic resonance on networks [1,2]. For example, Ref. [3] uses a master equation approach while Refs. [4,5] consider the noise-induced switching of bistable nodes in complex networks. Much of this work aims to explain the properties of attracting (statistically steady) states perturbed by noise; nonetheless, many important questions are related to the transient dynamics of networks affected by noise.

We consider transient noise-induced behavior in a network of asymmetric bistable attractor systems, where noise induces an effectively irreversible transition spread through coupling. Each node (corresponding to a subsystem) is assumed to have two states, a shallow, marginally stable mode (the “quiescent” state) and a deep, more stable mode (the “active” state) that is consequently more resistant to noise. We start with the system in the marginally stable mode and say it “escapes” when it crosses some threshold to the deeply stable mode. The time of first escape is a random variable that is jointly determined by the nonlinear dynamics and the noise process. The assumption of asymmetry means that escape from the deeper state occurs very rarely and so we can view the process as an irreversible cascade of escapes, similar to a cascade of toppling dominos. The coupling of the systems can promote (or hinder) the escape of others on the network and may cause certain sequences of escape to appear preferentially depending on coupling strength. In this paper we highlight that the timings and sequences of escapes are effectively “emergent properties” of the system, and we demonstrate that these properties can be usefully classed by coupling strength into qualitatively different regimes.

We consider an idealization of behavior that has been seen in a variety of applications. This includes: (a) signal propagation

by sequential switching between asymmetric stable states (observed experimentally in chains of bistable electronic circuits [6] or in cases where the bistability is noise induced [7]), (b) waves along unidirectionally coupled chains (or lattices) of bistable nodes with forcing at one end [8], (c) photoinduced phase transitions in spin-crossover materials with bistable dynamic potentials [9–11], (d) avalanches of gene activation in gene regulatory pathways to drive cell differentiation/development/cancer [12,13], or (e) cell fate in biofilm formation [14]. Other applications that could benefit from a better understanding of similar transient dynamics induced by noise include (a) the contagion of bank defaults in a system of financial institutions interconnected by mutual loans [15–18], (b) interconnections between “tipping elements” [19–21], (c) the role of spreading of abnormal large-amplitude oscillators in the modeling onset of epileptic seizures [22,23], (d) multiple organ failure [24], or (e) cascading failures in power systems [25].

The role of coupling strength in noise-induced transitions on networks is considered by Refs. [26,27] for idealized symmetric bistable systems. Neiman [28] shows similar synchronization effects in coupled stochastic bistable systems and Ref. [29] shows them in coupled ratchet systems. The authors of Refs. [26,27] give rigorous mathematical results that identify the existence of different regimes of synchronization of escapes in the low noise limit that can be linked to changes in the structure of the underlying system attractors (see, for example, Ref. [30] for some review of the role of coupling in the noise-free context). In particular, Ref. [26] identifies the most likely sequences of escape and how their probabilities change qualitatively with coupling strength: There can be synchronized transitions in the strong coupling limit. Many properties of the transitions can be understood using Friedlin-Wentzell methodology and the Eyring-Kramers formula [31–33] to study the pathwise properties of transitions between attractors.

We show in the context of asymmetric potentials that there are typically several qualitatively different regimes in the transient sequences of escapes. These regimes of

96 weak, intermediate, and strong coupling, and the intermediate  
 97 case may be quite complicated, but in general there are  
 98 qualitative changes in behavior for the weak noise limit that  
 99 can be characterized in terms of bifurcations of steady states of  
 100 the noise-free system. As a row of toppling dominos depends  
 101 on the properties and spacing of the dominos [34], we identify  
 102 different domino effects that can be characterized by different  
 103 coupling regimes. Specifically, we identify “slow domino”  
 104 and “fast domino” regimes corresponding to intermediate and  
 105 strong coupling regimes, respectively. Within these different  
 106 regimes, certain sequences of escape may be preferred by the  
 107 coupling, and the distribution of times to the next escape may  
 108 have significant deviations from the exponential.

## 109 II. SEQUENTIAL ESCAPES FOR TWO 110 COUPLED SYSTEMS

111 We consider a diffusively coupled network of prototypical  
 112 asymmetric bistable nodes under the influence of additive  
 113 noise for an asymmetric case of the Schlögl model [35]. For  
 114  $N = 2$  nodes and bidirectional coupling, there are qualitative  
 115 changes in the escape time distributions as the coupling  
 116 strength increases [36]. For  $N = 3$  nodes with unidirectional  
 117 coupling, we show that, although the mean and distributions of  
 118 the escape times of an individual node are not much affected  
 119 by the coupling, the probability of a given sequence appearing  
 120 and the distribution of timings within the sequence of escapes  
 121 can be greatly affected.

122 We consider a network where each node is governed by a  
 123 bistable system,

$$\dot{x} = f(x, v) := -(x - 1)(x^2 - v), \quad (1)$$

124 so that  $f = -V'(x)$  with potential  $V(x) = \frac{1}{4}x^4 - \frac{1}{3}x^3 +$   
 125  $v(x - \frac{1}{2}x^2)$ . We suppose that the nodes are coupled into a  
 126 network and subjected to additive noise. For  $0 < v \ll 1$  the  
 127 stable states are not interchangeable by any symmetry. There is  
 128 a quiescent attractor at  $x = x_Q := -\sqrt{v}$  and an active attractor  
 129 at  $x = x_A := 1$ ; there is an unstable separating equilibrium  
 130 at  $x = x_S := \sqrt{v}$ . Stationary distributions of this model are  
 131 examined in Ref. [35]. For nodes  $i = 1, \dots, N$  the network  
 132 is assumed to evolve according to the stochastic differential  
 133 equation (SDE),

$$dx_i = \left[ f(x_i, v) + \beta \sum_{j \in N_i} (x_j - x_i) \right] dt + \alpha dw_i, \quad (2)$$

134 where  $N_i$  are the neighbors that provide inputs to node  $i$ ,  $\beta$  is  
 135 the coupling strength,  $\alpha$  the strength of the additive noise, and  
 136  $w_i$  are independent Wiener processes.

137 In the case  $N = 2$  with bidirectional coupling [36], we have

$$\begin{aligned} dx_1 &= [f(x_1, v) + \beta(x_2 - x_1)]dt + \alpha dw_1, \\ dx_2 &= [f(x_2, v) + \beta(x_1 - x_2)]dt + \alpha dw_2, \end{aligned} \quad (3)$$

138 where in the noise-free case  $\alpha = 0$  there are equilibria at  
 139  $x_{QQ} := (x_Q, x_Q)$ ,  $x_{SS} := (x_S, x_S)$ , and  $x_{AA} := (x_A, x_A)$  for any  
 140  $\beta$ . Up to six more equilibria depend on  $0 \leq \beta$  and  $0 < v < 1$ .  
 141 The regimes noted in Ref. [36] can be precisely characterized.  
 142 One can verify that the number of solutions changes at a  
 143 saddle-node bifurcation when

$$-27\beta^3 + (27v + 9)\beta^2 - 9(v + \frac{1}{3})^2\beta + v(v - 1) = 0.$$

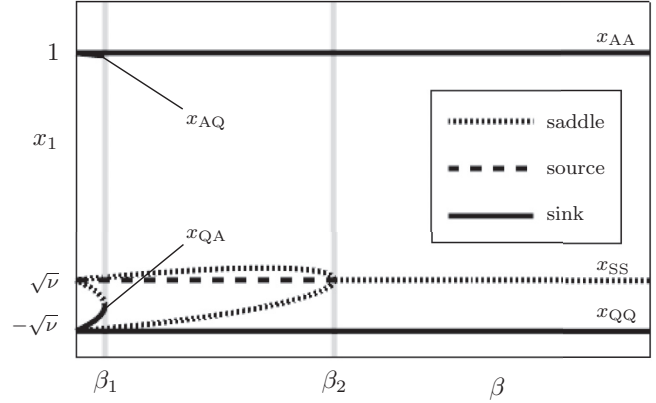


FIG. 1. Bifurcation diagram for the system of two bidirectionally coupled nodes (3) with  $\alpha = 0$  and  $v = 0.01$  projected into the  $(\beta, x_1)$  plane, where  $\beta$  is the coupling strength (cf. Fig. 2 in Ref. [36]). We are interested in how the system escapes from the quiescent attracting state  $x_{QQ}$  to the active attracting state  $x_{AA}$  under the influence of low-amplitude noise,  $0 < \alpha \ll 1$ . The three regimes that exist in terms of the structures that must be overcome for the transition have parallels in more general cases. In this case they are divided by a saddle-node (fold) bifurcation at  $\beta_1 = 0.0101$  and a pitchfork bifurcation of the separating saddles at  $\beta_2 = 0.09$ . In the weak coupling regime  $\beta < \beta_1$ , the escape will be via an additional attractor,  $x_{QA}$  or  $x_{AQ}$ , while in the strong coupling (“fast domino” regime)  $\beta > \beta_2$ , the escapes are approximately synchronized and pass near  $x_{SS}$ . Escapes in the intermediate coupling (“slow domino” regime)  $\beta_1 < \beta < \beta_2$  are associated with escape over a symmetry broken saddle.

For small  $v$  this implies there is a saddle node for  $\beta =$  144  
 $\beta_1 > 0$ . A pitchfork bifurcation occurs at intermediate  $\beta_2 =$  145  
 $(\sqrt{v} - 4v + 3v^{3/2})/(1 - 3\sqrt{v})$ . Let  $x_{QS}$  denote the branch of 146  
 equilibria that continues from  $(x_Q, x_S)$  at  $\beta = 0$ . We note 147  
 $x_{SA}$  (saddle) and  $x_{QA}$  (stable) meet while simultaneously  $x_{AS}$  148  
 (saddle) and  $x_{AQ}$  (stable) meet at the saddle node at  $\beta_1$ . The 149  
 branches  $x_{QS}$  and  $x_{SQ}$  meet  $x_{SS}$  at the pitchfork bifurcation 150  
 at  $\beta_2$ . Observe that there are three qualitatively different 151  
 regimes of coupling depending on whether there are nine 152  
 $(\beta < \beta_1)$ , five  $(\beta_1 < \beta < \beta_2)$ , or three  $(\beta > \beta_2)$  equilibria. 153  
 The bifurcation diagram for  $v = 0.01$  is shown in Fig. 1: in 154  
 this case,  $\beta_1 = 0.0101$  and  $\beta_2 = 0.09$ . 155

We give an initial condition  $x_i(0) = x_Q$  for (2) and pick a 156  
 threshold  $x_S < \xi < x_A$ . The first escape time of node  $i$  is the 157  
 random variable  $\tau^{(i)} = \inf\{t > 0 : x_i(t) > \xi\}$  that depends on 158  
 the network, the parameters, and the particular noise path: It 159  
 has a distribution implied by that of the noise. Independence 160  
 of the  $w_i$  means that (with probability one) no two escapes 161  
 will occur at the same time and so we can assume there is a 162  
 permutation  $s(i)$  of  $\{1, \dots, N\}$  such that  $\tau^{s(i)} < \tau^{s(j)}$  for any 163  
 $i < j$ . We denote by  $\mathbb{P}(s)$  the probability of a sequence  $s$  being 164  
 realized and define the time of the  $i$ th escape by  $\tau^i = \tau^{s(i)}$ . We 165  
 use the convention  $\tau^0 = 0$ . The time between escapes  $j$  and 166  
 $k > j$  is denoted  $\tau^{k|j} = \tau^k - \tau^j$ , with means  $T^{(i)} = \mathbb{E}[\tau^{(i)}]$  167  
 and  $T^{k|j} = \mathbb{E}[\tau^{k|j}]$ . Note that for  $\beta = 0$  all sequences are 168  
 equally likely, meaning  $\mathbb{P}(s) = 1/N!$ . 169

In networks of the form (3), as long as  $0 < v < 1$  so 170  
 that  $x_Q$  is linearly stable, the  $\tau^{(i)}$  are independent random 171  
 variables with exponential tails for  $\beta = 0$  whose mean can be 172

173 approximated using the one-dimensional Kramers' formula  
174 (e.g., Ref. [31]) which states in the limit  $\alpha \rightarrow 0$ ,

$$T^{(i)} \approx \frac{2\pi}{\sqrt{V''(x_Q)|V''(x_S)}} e^{\frac{2}{\alpha}[V(x_S)-V(x_Q)]}. \quad (4)$$

175 We show that the distributions  $\tau$  and  $\mathbb{P}(s)$  change in subtle  
176 ways on increasing  $\beta$ .

177 The persistence of the hyperbolic fixed points and the  
178 robustness of connections means there is a weak coupling  
179 regime. For small enough  $\beta > 0$ , the quiescent states are  
180 perturbed but not destroyed, and the escape of one node  
181 modifies the rate of escape of the other nodes. However, the  
182 means (4) should vary continuously with the parameter. For  
183 the strong coupling (synchronized) regime [26,28], for large  
184  $\beta$ , the nodes synchronize and there is a strong dependence,  
185 meaning they escape *en masse*, hence “fast domino.” For the  
186 intermediate coupling regime, the escape of one node leads  
187 to a delayed (but essentially deterministic) response from the  
188 other units, hence “slow domino.”

189 We illustrate these differences for (3) in Fig. 2, which  
190 shows the behavior of escapes from  $x_{QQ}$  in the weak noise  
191 limit with  $\nu = 0.01$  fixed and depending on  $\beta$ , where the  
192 SDE is solved using a fixed time-step Heun method. The  
193 symmetry in the coupling of the system can be seen as a  
194 reflection about the line  $x_1 = x_2$ . The coupled system (3) can  
195 be seen as a noise perturbed potential flow for  $\tilde{V}(x_1, x_2) =$   
196  $V(x_1) + V(x_2) + \frac{1}{2}\beta(x_1 - x_2)^2$  (we suppress the  $\nu$  and  $\beta$   
197 dependence). The mean escape time between two minima  
198 of the potential can be estimated using a multidimensional  
199 Kramers' formula: the mean time from  $x^*$  to  $y^*$  over the  
200 minimum height pass saddle (“gate”) at  $z^*$  is

$$T(x^*, z^*, y^*) \approx P(x^*, z^*) e^{\frac{2}{\alpha}[\tilde{V}(z^*) - \tilde{V}(x^*)]}$$

201 for  $\alpha \rightarrow 0$ , where the prefactor  $P$  depends on the Hessian  
202  $\nabla^2 \tilde{V}(z^*)$  (see, e.g., Ref. [31]). Note that to this leading order  
203  $T$  is independent of  $y^*$ .

204 We estimate the dependence of mean time  $T^{2|0} = T^{2|1} +$   
205  $T^{1|0}$  of escape for (3) on coupling, where there may be multiple  
206 paths of escape. If  $\tilde{T}(x^*, z^*, y^*)$  is the mean time of escape  
207 assuming it takes path  $\tilde{z}^*$  out of  $G$  possible symmetrically  
208 equivalent gates, then  $\tilde{T}(x^*, z^*, y^*) = \frac{1}{G} T(x^*, z^*, y^*)$ , where  $z^*$   
209 is associated with multiple paths of escape.

210 In the *weak coupling regime*  $0 < \beta < \beta_1$ , each symmetric  
211 path is equally probable and so  $2T^{1|0} \approx \tilde{T}(x_{QQ}, x_{QS}, x_{QA}) +$   
212  $\tilde{T}(x_{QQ}, x_{SQ}, x_{AQ})$ , while  $2T^{2|1} \approx T(x_{QA}, x_{SA}, x_{AA}) + T(x_{AQ},$   
213  $x_{AS}, x_{AA})$ . Hence

$$T^{2|0} \approx \frac{1}{2} T(x_{QQ}, x_{QS}, x_{QA}) + T(x_{QA}, x_{SA}, x_{AA}). \quad (5)$$

214 In the *intermediate coupling regime* (“slow domino”  
215 regime)  $\beta_1 < \beta < \beta_2$ , there is a one-step escape process, but  
216 there are two possible gates that can be traversed,

$$T^{2|0} \approx \frac{1}{2} [T(x_{QQ}, x_{SQ}, x_{AA}) + T(x_{QQ}, x_{QS}, x_{AA})]. \quad (6)$$

217 Note that this asymptotic expression will be nonuniform in  $\beta$ :  
218 near  $\beta = \beta_1$  there will be a long deterministic delay associated  
219 with passage past the region of the saddle node, as is evident  
220 in Fig. 2(c).

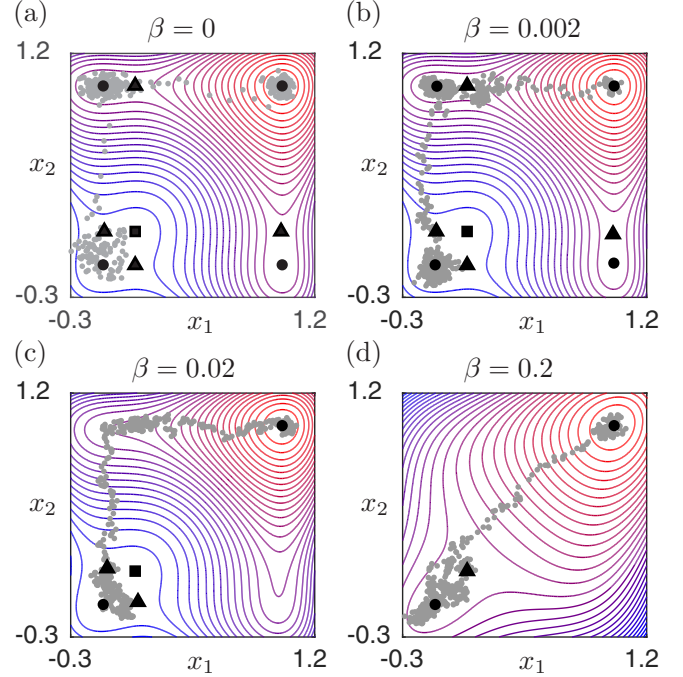


FIG. 2. Level sets of  $\tilde{V}$  (where red corresponds to the most negative) for  $N = 2$  bidirectionally coupled nodes (3) with fixed  $\nu = 0.05$  and four values of  $\beta$ . The equilibria for  $\alpha = 0$  are marked as  $\bullet$  sinks,  $\blacksquare$  sources, and  $\blacktriangle$  saddles. Typical noise paths starting at  $x_{QQ}$  are shown in each panel computed for (3) and for  $\alpha = 0.1$ . The panels show typical escapes of (a) uncoupled, (b) weakly coupled, (c) intermediate coupled (“slow domino”), and (d) strongly coupled (“fast domino”) regimes.

In the *strong coupling regime* (“fast domino” regime) 221  
 $\beta > \beta_2$ , there is a one-step escape process with a unique gate, 222

$$T^{2|0} \approx T(x_{QQ}, x_{SS}, x_{AA}). \quad (7)$$

Each of these regimes will give a different scaling in the limit 223  
 $\alpha \rightarrow 0$ , while the scalings at crossovers between regimes are 224  
accessible to generalizations of Kramers' formula for passage 225  
over nonhyperbolic saddles [31]. This is explored in more detail 226  
in Ref. [37], including computing the timing of the escape once 227  
the gate has been traversed in the intermediate and strong coupling 228  
regimes. 229

### III. SEQUENTIAL ESCAPES FOR A THREE NODE CHAIN 230

For a more general network, the sequence of escapes of the 231  
network depends not only on the number of nodes that have 232  
already escaped but also the sequence in which they escape. We 233  
consider a unidirectionally coupled chain of  $N = 3$  bistable 234  
systems (2) where the input sets  $N_i$  for node  $i$  are given by 235  
 $(N_1, N_2, N_3) = (\{2\}, \{3\}, \{\})$ , 236

$$\begin{aligned} dx_1 &= [f(x_1, v) + \beta(x_2 - x_1)]dt + \alpha dw_1, \\ dx_2 &= [f(x_2, v) + \beta(x_3 - x_2)]dt + \alpha dw_2, \\ dx_3 &= [f(x_3, v)]dt + \alpha dw_3. \end{aligned} \quad (8)$$

Figure 3 illustrates the three coupling regimes: the weak cou- 237  
pling regime ( $\beta < \beta_1$ ), intermediate coupling (slow domino) 238  
( $\beta_1 < \beta < \beta_3$ ), and strong coupling (fast domino) ( $\beta > \beta_3$ ) 239



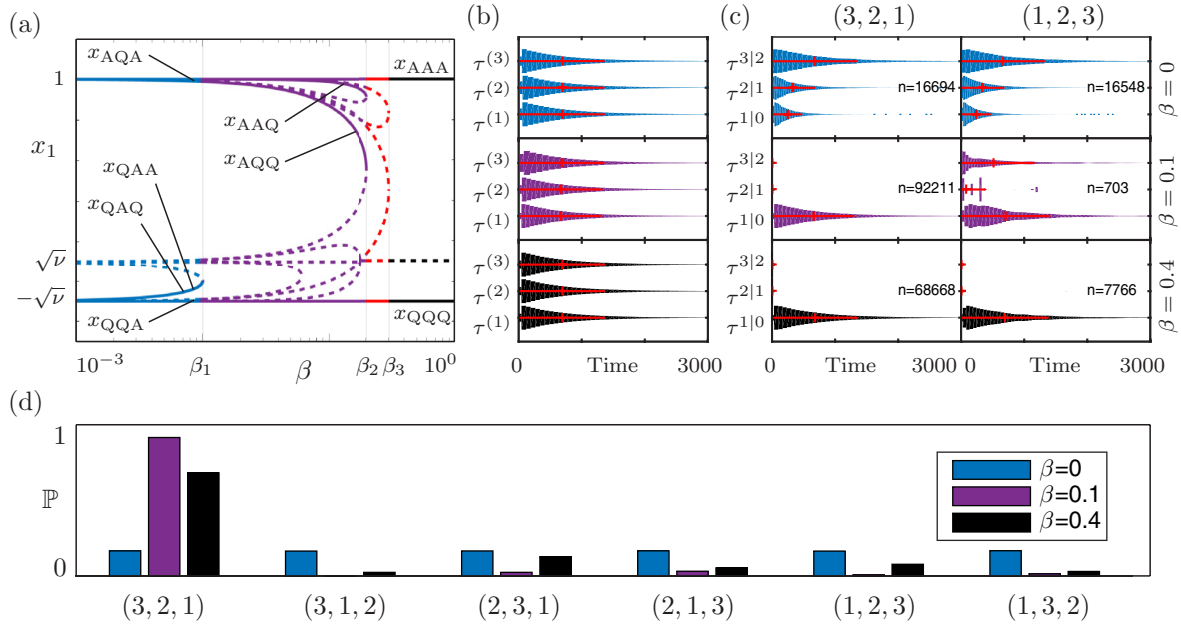


FIG. 3. (a) Bifurcation diagram showing  $x_1$  vs  $\beta$  (log axis) for (8) with  $\nu = 0.01$  and no noise  $\alpha = 0$ : Dashed branches are unstable. In the weak coupling regime ( $\beta < \beta_1 = 0.0101$ , blue) all branches continue from  $\beta = 0$ . There are two intermediate (slow domino) coupling regimes: For the lower one ( $\beta_1 < \beta < \beta_2 \approx 0.2025$ , purple) there are still stable and unstable partially escaped states while for ( $\beta_2 < \beta < \beta_3 \approx 0.3035$ , red) there are only partially escaped saddles. For the strong (fast domino) coupling regime  $\beta > \beta_3$ , all equilibria are synchronized in the absence of noise. For (b)–(d) we computed  $10^5$  samples using  $\alpha = 0.03$  for  $\beta = 0$  (blue), 0.1 (purple), and 0.4 (black). (b) shows violin plots of the distribution of escape times  $\tau^{(i)}$  of node  $i$ : Observe that these change little with coupling. The red cross indicates mean (vertical) and  $\pm$  one standard deviation (horizontal). (c) shows the distribution of sequential escape times  $\tau^{k|k-1}$  for  $k = 1, 2, 3$ , for sequences (3, 2, 1) and (1, 2, 3). The number of samples  $n$  (out of  $10^5$ ) that undergo this sequence of escapes is shown. (d) shows the probability of a given sequence being realized. In the strongly coupled case  $\beta = 0.4$ , the escapes are almost always synchronized, and the most frequent sequence is (3, 2, 1). The case  $\beta = 0.1$  and sequence (1, 2, 3) is an example of a nonsynchronous escape in the intermediate coupling regime; the third escape typically occurs some time after the first two: see Table I.

regimes for this system. Note that intermediate coupling can be split further into two subregimes at  $\beta_2$ . There are qualitative changes in the asymptotic behavior of sequential escapes on changing  $\beta$ , with strongly synchronized escapes for strong coupling.

To characterize the distribution of times of  $n$ th escape we consider the coefficient of variation of  $\tau$  given by

$$\text{CV}(\tau) = \sigma(\tau)/\mathbb{E}[\tau],$$

where  $\sigma(\tau)$  denotes the standard deviation. For  $\beta = 0.0$  (and for all first escapes) we have  $\text{CV}(\tau^{k|k-1}) \approx 1$ , indicating an exponential distribution. In the intermediate coupling (slow domino) regime  $\beta = 0.1$ , the most likely sequence is (3, 2, 1): Considering only this sequence for the data in Fig. 3, we find  $\text{CV}(\tau^{1|0}) = 0.9608$ ,  $\text{CV}(\tau^{2|1}) = 0.3308$ , and  $\text{CV}(\tau^{3|2}) = 0.2210$ —after the first (approximately exponentially distributed) escape the remaining escapes are close to deterministic ( $\mathbb{E}[\tau^{2|1}] = 4.087$ ,  $\mathbb{E}[\tau^{3|2}] = 4.797$ ). On the other hand, for a rarer sequence (1, 2, 3) in the intermediate regime, we find  $\text{CV}(\tau^{1|0}) = 0.9783$ ,  $\text{CV}(\tau^{2|1}) = 3.662$ , and  $\text{CV}(\tau^{3|2}) = 1.27$ —after the first exponentially distributed escape there are very large variations in escape time. Finally, in the strongly coupling (fast domino) regime  $\beta = 0.4$  and the most likely sequence (3, 2, 1), we have  $\mathbb{E}[\tau^{2|1}] = 0.6568$ ,  $\mathbb{E}[\tau^{3|2}] = 0.9664$ . Table I gives the probability, mean, and coefficient of variation for sequential escape times of the

simulations shown in Fig. 3. Note that as  $\beta$  increases, the system remains closer to synchronization, leading to an increasing randomization of the sequence of escapes caused by fluctuations about the synchronized state.

#### IV. DISCUSSION

For general heterogeneous networks it is still possible to classify the interactions between nodes  $x_i$  and  $x_j$  as weak, intermediate, or strong depending on whether the escape of node  $x_i$  modifies the rate of the noise-induced escape of  $x_j$ , whether  $x_j$  will undergo a deterministic escape in a bounded time, or whether  $x_j$  will be synchronized in its escape with  $x_i$ , respectively. This will depend on the state of the other nodes that are connected to  $x_i$  and  $x_j$ , and so the classification of the interaction is, in general, state and sequence dependent.

The changes in distribution of timings and sequences of escapes in stochastically perturbed coupled networks can be usefully thought of as an emergent behavior of the network. In particular, even for intermediate or strong coupling where there are no symmetry broken attractors in the noise-free case, the asymptotic behavior of the sequence of escapes is qualitatively different in the low noise limit. A study of such sequential escapes will be of interest in a variety of situations where stochastic forcing of individual sites with asymmetric attractors interacts with the coupling strength to change the sequence of escapes. For example, Ref. [37] uses

TABLE I. Data table. For the simulations shown in Fig. 3, the columns in this table show the sequence of escape, the probability  $\mathbb{P}$  that a sequence will be realized, followed by the mean, standard deviation, and coefficient of variation of  $\tau^{k|k-1}$  conditional on this sequence for  $k = 1, 2, 3$ .

Sequence	$\mathbb{P}$	$\tau$	$\mathbb{E}(\tau)$	$\sigma(\tau)$	$\text{CV}(\tau)$	$\tau$	$\mathbb{E}(\tau)$	$\sigma(\tau)$	$\text{CV}(\tau)$	$\tau$	$\mathbb{E}(\tau)$	$\sigma(\tau)$	$\text{CV}(\tau)$
$\beta = 0$ : Uncoupled systems													
(3,2,1)	0.167	$\tau^{1 0}$	244.53	221.98	0.91	$\tau^{2 1}$	334.87	340.60	1.02	$\tau^{3 2}$	673.07	668.26	0.99
(3,1,2)	0.166	$\tau^{1 0}$	245.94	222.72	0.91	$\tau^{2 1}$	333.61	330.46	0.99	$\tau^{3 2}$	662.49	661.12	1.00
(2,3,1)	0.167	$\tau^{1 0}$	246.58	226.22	0.92	$\tau^{2 1}$	332.64	329.08	0.99	$\tau^{3 2}$	668.02	674.47	1.01
(2,1,3)	0.167	$\tau^{1 0}$	243.26	223.67	0.92	$\tau^{2 1}$	334.81	331.77	0.99	$\tau^{3 2}$	671.92	665.28	0.99
(1,2,3)	0.165	$\tau^{1 0}$	243.57	223.05	0.92	$\tau^{2 1}$	337.94	337.15	1.00	$\tau^{3 2}$	664.35	655.76	0.99
(1,3,2)	0.168	$\tau^{1 0}$	246.26	224.39	0.91	$\tau^{2 1}$	329.51	329.09	1.00	$\tau^{3 2}$	667.31	667.83	1.00
$\beta = 0.1$ : Intermediate coupling regime (“slow domino-effect”)													
(3,2,1)	0.922	$\tau^{1 0}$	658.98	633.17	0.96	$\tau^{2 1}$	4.09	1.36	0.33	$\tau^{3 2}$	4.80	1.06	0.22
(3,1,2)	0.002	$\tau^{1 0}$	730.13	658.49	0.90	$\tau^{2 1}$	2.26	1.42	0.63	$\tau^{3 2}$	1.12	1.01	0.90
(2,3,1)	0.024	$\tau^{1 0}$	652.22	611.87	0.94	$\tau^{2 1}$	1.50	1.27	0.85	$\tau^{3 2}$	2.97	1.55	0.52
(2,1,3)	0.031	$\tau^{1 0}$	666.43	647.67	0.97	$\tau^{2 1}$	3.54	1.70	0.48	$\tau^{3 2}$	487.84	673.65	1.38
(1,2,3)	0.007	$\tau^{1 0}$	704.30	689.06	0.98	$\tau^{2 1}$	82.71	302.97	3.66	$\tau^{3 2}$	509.47	647.88	1.27
(1,3,2)	0.014	$\tau^{1 0}$	703.84	663.34	0.94	$\tau^{2 1}$	617.64	665.10	1.08	$\tau^{3 2}$	3.93	1.46	0.37
$\beta = 0.4$ : Strong coupling regime (“fast domino-effect”)													
(3,2,1)	0.687	$\tau^{1 0}$	688.02	662.25	0.96	$\tau^{2 1}$	0.66	0.38	0.58	$\tau^{3 2}$	0.97	0.40	0.41
(3,1,2)	0.024	$\tau^{1 0}$	708.41	691.41	0.98	$\tau^{2 1}$	0.36	0.27	0.75	$\tau^{3 2}$	0.21	0.18	0.86
(2,3,1)	0.128	$\tau^{1 0}$	690.46	682.03	0.99	$\tau^{2 1}$	0.29	0.25	0.86	$\tau^{3 2}$	0.62	0.39	0.63
(2,1,3)	0.053	$\tau^{1 0}$	702.68	681.17	0.97	$\tau^{2 1}$	0.41	0.31	0.76	$\tau^{3 2}$	0.50	0.53	1.06
(1,2,3)	0.078	$\tau^{1 0}$	695.96	680.09	0.98	$\tau^{2 1}$	4.00	49.62	12.41	$\tau^{3 2}$	0.76	0.70	0.92
(1,3,2)	0.030	$\tau^{1 0}$	694.73	651.60	0.94	$\tau^{2 1}$	17.54	151.01	8.61	$\tau^{3 2}$	0.30	0.24	0.80

289 this to explain some phenomena in the networks of coupled  
290 oscillatory bistable units considered in Ref. [22].

### ACKNOWLEDGMENTS

291  
292 The authors gratefully acknowledge the financial sup-  
293 port of the EPSRC via Grant No. EP/N014391/1. We

294 thank the anonymous referees for their comments, criti-  
295 cisms, and suggestions. P.A. gratefully acknowledges fund-  
296 ing from the European Union’s Horizon 2020 research  
297 and innovation programme under the Marie Skłodowska-  
298 Curie Grant Agreement No. 643073 for providing opportu-  
299 nities to discuss this work with members of the CRITICS  
300 network.

- [1] P. Jung, U. Behn, E. Pantazelou, and F. Moss, Collective response in globally coupled bistable systems, *Phys. Rev. A* **46**, R1709 (1992).
- [2] A. Pikovsky, A. Zaikin, and M. A. de La Casa, System Size Resonance in Coupled Noisy Systems and in the Ising Model, *Phys. Rev. Lett.* **88**, 050601 (2002).
- [3] S. Christ, B. Sonnenschein, and L. Schimansky-Geier, Tristable and multiple bistable activity in complex random binary networks of two-state units, *Eur. Phys. J. B* **90**, 14 (2017).
- [4] G. Ansmann, K. Lehnertz, and U. Feudel, Self-Induced Switchings Between Multiple Space-Time Patterns on Complex Networks of Excitable Units, *Phys. Rev. X* **6**, 011030 (2016).
- [5] J. Emenheiser, A. Chapman, M. Pósfai, J. P. Crutchfield, M. Mesbahi, and R. M. D’Souza, Patterns of patterns of synchronization: Noise induced attractor switching in rings of coupled nonlinear oscillators, *Chaos* **26**, 094816 (2016).
- [6] M. Löcher, D. Cigna, and E. R. Hunt, Noise Sustained Propagation of a Signal in Coupled Bistable Electronic Elements, *Phys. Rev. Lett.* **80**, 5212 (1998).
- [7] A. A. Zaikin, J. García-Ojalvo, L. Schimansky-Geier, and J. Kurths, Noise Induced Propagation in Monostable Media, *Phys. Rev. Lett.* **88**, 010601 (2001).
- [8] J. F. Lindner, S. Chandramouli, A. R. Bulsara, M. Löcher, and W. L. Ditto, Noise Enhanced Propagation, *Phys. Rev. Lett.* **81**, 5048 (1998).
- [9] K. Boukheddaden, I. Shteto, B. Hôo, and F. Varret, Dynamical model for spin-crossover solids. II. Static and dynamic effects of light in the mean-field approach, *Phys. Rev. B* **62**, 14806 (2000).
- [10] T. Ogawa, Domino mechanisms in photoinduced phase transitions, *Phase Trans.* **74**, 93 (2001).
- [11] K. Yonemitsu and K. Nasu, Theory of photoinduced phase transitions in itinerant electron systems, *Phys. Rep.* **465**, 1 (2008).
- [12] T. Graf and T. Enver, Forcing cells to change lineages, *Nature (London)* **462**, 587 (2009).
- [13] J. Wang, L. Xu, E. Wang, and S. Huang, The potential landscape of genetic circuits imposes the arrow of time in stem cell differentiation, *Biophys. J.* **99**, 29 (2010).

- [14] Y. Chai, F. Chu, R. Kolter, and R. Losick, Bistability and biofilm formation in *Bacillus subtilis*, *Mol. Microbiol.* **67**, 254 (2008).
- [15] M. Chinazzi and G. Fagiolo, Systemic risk, contagion, and financial networks: A survey, SSRN, doi:[10.2139/ssrn.2243504](https://doi.org/10.2139/ssrn.2243504) (2013).
- [16] P. Gai and S. Kapadia, Contagion in financial networks, *Proc. R. Soc. London Ser. A* **466**, 2401 (2010).
- [17] A. G. Haldane and R. M. May, Systemic risk in banking ecosystems, *Nature (London)* **469**, 351 (2011).
- [18] M. Summer, Financial contagion and network analysis, *Annu. Rev. Financ. Econ.* **5**, 277 (2013).
- [19] P. Ashwin, S. Wicczorek, R. Vitolo, and P. Cox, Tipping points in open systems: Bifurcation, noise-induced and rate-dependent examples in the climate system, *Philos. Trans. R. Soc. A* **370**, 1166 (2012); C. Hobbs, P. Ashwin, S. Wicczorek, R. Vitolo, and P. Cox, *ibid.* **371**, 0098 (2013)
- [20] T. M. Lenton, H. Held, E. Kriegler, J. W. Hall, W. Lucht, S. Rahmstorf, and H. J. Schellenhuber, Tipping elements in the earth's climate system, *Proc. Natl. Acad. Sci. USA* **105**, 1786 (2008).
- [21] C. A. Boulton, L. C. Allison, and T. M. Lenton, Early warning signals of atlantic meridional overturning circulation collapse in a fully coupled climate model, *Nat. Commun.* **5**, 5752 (2014).
- [22] O. Benjamin, T. H. B. Fitzgerald, P. Ashwin, K. Tsaneva-Atanasova, F. Chowdhury, M. P. Richardson, and J. R. Terry, A phenomenological model of seizure initiation suggests network structure may explain seizure frequency in idiopathic generalised epilepsy, *J. Math. Neurosci.* **2**, 1 (2012).
- [23] S. N. Kalitzin, D. N. Velis, and F. H. Lopes da Silva, Stimulation-based anticipation and control of state transitions in the epileptic brain, *Epilepsy Behav.* **17**, 310 (2010).
- [24] R. S. Parker and G. Clermont, Systems engineering medicine: engineering the inflammation response to infectious and traumatic challenges, *J. R. Soc. Interface* **7**, 989 (2010).
- [25] I. Dobson, B. A. Carreras, V. E. Lynch, and D. E. Newman, Complex systems analysis of series of blackouts: Cascading failure, critical points, and self-organization, *Chaos* **17**, 026103 (2007).
- [26] N. Berglund, B. Fernandez, and B. Gentz, Metastability in interacting nonlinear stochastic differential equations: I. From weak coupling to synchronization, *Nonlinearity* **20**, 2551 (2007).
- [27] N. Berglund, B. Fernandez, and B. Gentz, Metastability in interacting nonlinear stochastic differential equations: II. Large- $N$  behavior, *Nonlinearity* **20**, 2583 (2007).
- [28] A. Neiman, Synchronizationlike phenomena in coupled stochastic bistable systems, *Phys. Rev. E* **49**, 3484 (1994).
- [29] J. L. Mateos and F. R. Alariste, Phase synchronization for two Brownian motors with bistable coupling on a ratchet, *Chem. Phys.* **375**, 464 (2010).
- [30] *Dynamics of Coupled Map Lattices and of Related Spatially Extended Systems*, edited by J.-R. Chazottes and B. Fernandez, Lecture Notes in Physics Vol. 671 (Springer, New York, 2005).
- [31] N. Berglund, Kramers' law: Validity, derivations and generalisations, *Markov Processes Relat. Fields* **19**, 459 (2013), [arXiv:1106.5799](https://arxiv.org/abs/1106.5799).
- [32] N. Berglund and B. Gentz, *Noise-Induced Phenomena in Slow-Fast Dynamical Systems*, Springer Series on Probability and its Applications (Springer, Berlin, 2006).
- [33] H. A. Kramers, Brownian motion in a field of force and the diffusion model of chemical reactions, *Physica* **7**, 284 (1940).
- [34] J. M. J. Van Leeuwen, The domino effect, *Am. J. Phys.* **78**, 721 (2010).
- [35] H. Malchow, W. Ebeling, R. Feistel, and L. Schimansky-Geier, Stochastic bifurcations in a bistable reaction-diffusion system with Neumann boundary conditions, *Ann. Phys.* **495**, 151 (1983).
- [36] M. Frankowicz and E. Gudowska-Nowak, Stochastic simulation of a bistable chemical system: The two-box model, *Physica A* **116**, 331 (1982).
- [37] J. L. Creaser, K. Tsaneva-Atansova, and P. Ashwin, Sequential noise-induced escapes for oscillatory network dynamics, *SIAM J. Appl. Dyn. Syst.* (2017), [arXiv:1705.08462](https://arxiv.org/abs/1705.08462).